American Journal of Pathology, Vol. 165, No. 5, November 2004

Tumorigenesis and Neoplastic Progression

Quantitative Gene Expression Profiling in Formalin-Fixed, Paraffin-Embedded Tissues Using Universal Bead Arrays

Marina Bibikova,* Dimitri Talantov,† Eugene Chudin,* Joanne M. Yeakley,* Jing Chen,* Dennis Doucet,* Eliza Wickham,* David Atkins,† David Barker,* Mark Chee,* Yixin Wang,† and Jian-Bing Fan*

From Illumina, Inc., San Diego; and Veridex, LLC,† a Johnson & Johnson Company, San Diego, California*

We recently developed a sensitive and flexible gene expression profiling system that is not dependent on an intact poly-A tail and showed that it could be used to analyze degraded RNA samples. We hypothesized that the DASL (cDNA-mediated annealing, selection, extension and ligation) assay might be suitable for the analysis of formalin-fixed, paraffin-embedded tissues, an important source of archival tissue material. We now show that, using the DASL assay system, highly reproducible tissue- and cancer-specific gene expression profiles can be obtained with as little as 50 ng of total RNA isolated from formalin-fixed tissues that had been stored from 1 to over 10 years. Further, tissue- and cancer-specific markers derived from previous genome-wide expression profiling studies of fresh-frozen samples were validated in the formalin-fixed samples. The DASL assay system should prove useful for high-throughput expression profiling of archived clinical samples. ***(Am J Pathol 2004, 165:1799–1807)***

The recent development of high-throughput microarray technologies provides a powerful tool for genome-wide gene expression analysis.[1] For example, microarray-based tumor classification,[2–4] as well as treatment response and clinical outcome prediction,[4–7] have been demonstrated in many cancer types. However, these technologies typically require substantial quantities of fresh or frozen tissue. Although many institutions are now maintaining frozen tissue banks, which should facilitate gene expression analysis in the future, few of these now have sufficient clinical follow-up data. On the other hand, there is a vast supply of formalin-fixed, paraffin-embedded (FFPE) tissues for which the clinical outcome is already known.[8] The ability to analyze gene expression patterns in these archived tissues would greatly facilitate retrospective studies to correlate gene expression patterns with given disease states, or histological and clinical phenotypes. This approach could be used to discover biomarkers for therapeutic decision making and also to develop clinical tests, as FFPE sample collection and storage is a routine practice in pathology laboratories.

A barrier to the analysis of FFPE samples is that RNA extracted from FFPE tissues is often significantly degraded. Previous studies show that only about 3% or less of the RNA isolated from paraffin samples is accessible to cDNA synthesis, compared to fresh-frozen samples.[9] In particular, this has impeded progress in microarray-based gene expression quantitation from FFPE specimens.[10] As a result, most gene expression analysis of FFPE tissues has so far been done using immunohistochemical staining (IHC) and quantitative RT-PCR (qPCR), which allow only a few genes to be analyzed at a time.[9,11–16] Although sufficient RNA can be isolated from a few 10-μm slide-mounted paraffin sections to quantitate up to 30 genes by qPCR,[17] there is clearly a bottleneck in scaling up the number of genes that can be measured by this approach. Also, qPCR does not reliably measure RNA fragments shorter than 100 bp.[17]

We have recently developed a flexible, sensitive, and reproducible gene expression profiling assay, DASL (cDNA-mediated annealing, selection, extension and ligation), for parallel analysis of hundreds of genes with as little as 25 ng of total RNA.[18] We hypothesized that the DASL assay might be able to overcome the technical limitations to microarray-based analysis of FFPE samples. While most array technologies use an *in vitro* transcription (IVT)-mediated sample labeling procedure,[19]

Supported in part by grant R33 CA88351 from the National Institutes of Health.

Supplemental information can be found at http://ajp.amjpathol.org.

Accepted for publication July 6, 2004.

Address reprint requests to Jian-Bing Fan, Genetic Analysis, Illumina, Inc., 9885 Towne Center Drive, San Diego, CA 92121. E-mail: jfan@illumina.com.

DASL uses random priming in the cDNA synthesis, and therefore does not depend on an intact poly-A tail for oligo-d(T) priming. In addition, the assay requires a relatively short target sequence of about 50 nucleotides for query oligonucleotide annealing. In this study, we characterized the sensitivity and quantitative performance of the assay system on FFPE tissues and demonstrated its utility for marker validation as well as new marker identification. The results show that the DASL assay is effective for an important and extensive source of archival clinical material that was hitherto largely inaccessible to microarray technology. This opens up new avenues to the large-scale discovery, validation, and clinical application of mRNA biomarkers of disease.

Materials and Methods

Tissue Specimens

Sample set consisted of 11 matched pairs of FFPE colon cancer and adjacent normal tissues, and 11 matched pairs of FFPE breast cancer and adjacent normal tissues. Colon cancer tissue specimens included 2 Dukes B1 (both well differentiated adenocarcinomas), 5 Dukes B2 (4 moderately and 1 well differentiated adenocarcinoma) and 4 Dukes C2 (2 well, 1 moderately differentiated, and 1 mucinous adenocarcinoma). Breast cancer tissue specimens included one Stage 0, two Stage I, six Stage IIA, one Stage IIB, and one Stage IIIC. There were nine infiltrative ductal carcinomas, one mucinous carcinoma and one ductal carcinoma *in situ*. Colon cancer was staged according to Modified Aston-Coller classification and breast cancer was staged according to AJCC Cancer Staging Manual (Sixth Edition, Springer, 2003). All samples were obtained from Asterand, Inc. (Detroit, MI) according to an Institutional Review Board approved protocol. Patient demographic and pathology information was also collected. Among the eleven sample pairs of each tissue type, four pairs were collected in a period within 1 year, four pairs in a period of 2 years, and three pairs in a period of 9 to 11 years before the current study (Table 1). Along with the FFPE samples, two matched pairs of fresh-frozen colon cancer and adjacent normal tissue and two matched pairs of fresh-frozen breast cancer and adjacent normal tissue were collected from the patients included in the FFPE sample set. The histopathological features of each sample were reviewed to confirm diagnosis and tumor content.

RNA Isolation

For total RNA isolation from FFPE tissues, three 20-μm-thick sections were cut from each tissue block. The High Pure RNA Paraffin Kit (Roche) was used. Proteinase K digestion time was 12 hours for each sample. All purification, DNase treatment, and other steps were performed according to the manufacturer's protocol. After total RNA isolation, samples were stored at −80°C until use.

Total RNA from fresh-frozen tissue samples was isolated by a standard Trizol/chloroform method. Tissue was homogenized in Trizol reagent (Invitrogen). Total RNA was isolated from Trizol and precipitated at −20°C with isopropyl alcohol. RNA pellets were washed with 75% ethanol, dissolved in water, and stored at −80°C until use. RNA integrity was examined with the Agilent 2100 Bioanalyzer RNA 6000 Nano Assay (Agilent Technologies).

Real-Time Qantitative RT-PCR (qPCR)

qPCR analyses were performed on the ABI Prism 7900HT sequence detection system (Applied Biosystems) as described previously.[18] Most PCR primers were designed to amplify approximately 90-bp fragments. Primers for the RPL13A transcript were designed to amplify 90-bp and 155-bp fragments.

BeadArray Manufacture

Microarrays were assembled by loading pools of glass beads (3 μm in diameter) derivatized with oligonucleotides onto the etched ends of fiber-optic bundles.[20] About 50,000 optical fibers are hexagonally packed to form a ~1.4 mm diameter bundle. The fiber optic bundles are assembled into an array matrix (Sentrix array), comprising 96 bundles arranged in an 8 × 12 matrix that matches the dimensions of standard microtiter plates.[21] This arrangement allows simultaneous processing of 96 samples using standard robotics. Because the beads are positioned randomly, a decoding process is carried out to determine the location and identity of each bead in every array location.[22] Decoding is an automated part of array manufacture.

Assay Probe Design

For array analysis, two probe oligonucleotides were designed to interrogate each target site on the cDNA as described previously,[18] with 2 to 10 target sites per gene (average 6 sites). The first oligo consists of two parts: the gene-specific sequence and a universal PCR primer sequence (P1, 5′-ACTTCGTCAGTAACGGAC-3′) at the 5′-end. The second oligo consists of three parts: the gene-specific sequence, a unique address sequence which is complementary to one of 1520 capture sequences on the array, and a universal PCR primer sequence (P2, 5′-GTCTGCCTATAGTGAGTC-3′) at the 3′-end. A single address sequence is uniquely associated with a single target site. This address sequence allows the PCR-amplified products (see below) to hybridize to a universal microarray bearing the complementary probe sequences.[21] The gene-specific sequence is designed with Tm ranging from 57°C to 62°C.

Array Analysis

cDNA synthesis, DASL process, array image processing, and signal extraction were as described previously.[18] First, a 20-μl reverse transcription reaction containing a reaction mix (MMC; Illumina, San Diego, CA), biotinylated

Table 1. Tissue Samples

Sample ID*	Surgery year	Sample type	Diagnosis	Clinical stage	TNM†
FS1_CC2	2002	Frozen	Mucinous adenocarcinoma	Dukes C2	T4N1M0
FS1_CN2			Normal		
FS1_CC4	2002	Frozen	Moderately differentiated adenocarcinoma	Dukes C2	T3N1M0
FS1_CN4			Normal		
FS1_BC2	2002	Frozen	Infiltrating ductal carcinoma	Stage I	T1N0M0
FS1_BN2			Normal		
FS1_BC3	2002	Frozen	Infiltrating ductal carcinoma	Stage IIA	T2N0M0
FS1_BN3			Normal		
FS1_CC1	2002	FFPE	Well differentiated adenocarcinoma	Dukes B2	T3N0Mx
FS1_CN1			Normal		
FS1_CC2	2002	FFPE	Mucinous adenocarcinoma	Dukes C2	T4N1M0
FS1_CN2			Normal		
FS1_CC3	2002	FFPE	Well differentiated adenocarcinoma	Dukes B1	T2N0M0
FS1_CN3			Normal		
FS1_CC4	2002	FFPE	Moderately differentiated adenocarcinoma	Dukes C2	T3N1M0
FS1_CN4			Normal		
FS2_CC1	2001	FFPE	Well differentiated adenocarcinoma	Dukes B1	T2N0M0
FS2_CN1			Normal		
FS2_CC2	2001	FFPE	Well differentiated adenocarcinoma	Dukes C2	T3N1M0
FS2_CN2			Normal		
FS2_CC3	2001	FFPE	Moderately differentiated adenocarcinoma	Dukes B2	T4N0M0
FS2_CN3			Normal		
FS2_CC4	2001	FFPE	Well differentiated adenocarcinoma	Dukes C2	T3N1M0
FS2_CN4			Normal		
FS3_CC1	1994	FFPE	Moderately differentiated adenocarcinoma	Dukes B2	T3N0M0
FS3_CN1			Normal		
FS3_CC2	1992	FFPE	Moderately differentiated adenocarcinoma	Dukes B2	T3N0M0
FS3_CN2			Normal		
FS3_CC3	1994	FFPE	Moderately differentiated adenocarcinoma	Dukes B2	T3N0Mx
FS3_CN3			Normal		
FS1_BC1	2002	FFPE	Mucinous adenocarcinoma	Stage IIA	T2N0M0
FS1_BN1			Normal		
FS1_BC2	2002	FFPE	Infiltrating ductal carcinoma	Stage I	T1N0M0
FS1_BN2			Normal		
FS1_BC3	2002	FFPE	Infiltrating ductal carcinoma	Stage IIA	T2N0M0
FS1_BN3			Normal		
FS1_BC4	2002	FFPE	Infiltrating ductal carcinoma	Stage IIB	T2N1M0
FS1_BN4			Normal		
FS2_BC1	2001	FFPE	Infiltrating ductal carcinoma	Stage IIA	T2N0M0
FS2_BN1			Normal		
FS2_BC2	2001	FFPE	Infiltrating ductal carcinoma	Stage I	T1N0M0
FS2_BN2			Normal		
FS2_BC3	2001	FFPE	Infiltrating ductal carcinoma	Stage IIIC	T2N3M0
FS2_BN3			Normal		
FS2_BC4	2001	FFPE	Infiltrating ductal carcinoma	Stage IIIA	T2N2M0
FS2_BN4			Normal		
FS3_BC1	1993	FFPE	Infiltrating ductal carcinoma	Stage IIA	T2N0M0
FS3_BN1			Normal		
FS3_BC2	1993	FFPE	Infiltrating ductal carcinoma	Stage IIA	T2N0M0
FS3_BN2			Normal		
FS3_BC3	1993	FFPE	Ductal carcinoma *in situ*	Stage 0	TisN0M0
FS3_BN3			Normal		

*CC, colon cancer; CN, colon normal; BC, breast cancer; BN, breast normal.
†Tumor classification scale.

random hexamers and oligo-d(T)$_{18}$, and total RNA (up to 1 μg), was incubated at room temperature for 10 minutes and then at 42°C for 1 hour. The oligo-d(T) priming helps improve assay sensitivity for fresh-frozen samples with intact RNA. Pooled assay oligos were annealed to their sequence-specific targets on the cDNA under a controlled hybridization program.[21] The cDNA was immobilized on paramagnetic beads and washed to remove any excess or mis-hybridized oligos. Hybridized oligos were then extended and ligated to generate amplifiable templates, using Illumina-supplied reagents and conditions (BeadStation User's Manual, Illumina). A PCR reaction was performed with Cy3 labeled universal PCR primers. Single-stranded PCR products were prepared by denaturation, and were then hybridized to Sentrix arrays under a temperature gradient program.[21] The arrays were imaged using a BeadArray Reader scanner (Illumina).[20] Image processing and intensity data extraction software were as describe previously.[23] The DASL assay was performed three times independently, and samples were hybridized to three different array matrices. The sample and array coordinate information is shown in Table 2. All

Table 2. Sample and Array Coordinates

Sample ID*	Array matrix 1		Array matrix 2		Array matrix 3	
	Samples†	R^2 correlation‡	Samples	R^2 correlation	Samples	R^2 correlation
FS1_CC2_FF	+	0.989			+	0.991
FS1_CN2_FF	+	0.989			+	0.982
FS1_CC4_FF			+	0.997	+	0.985
FS1_CN4_FF			+	0.994	+	0.976
FS1_BC2_FF	+	0.991			+	0.996
FS1_BN2_FF	+	0.979			+	0.978
FS1_BC3_FF			+	0.994	+	0.990
FS1_BN3_FF			+	0.992	+	0.962
FS1_CC1	+	0.990			+	0.978
FS1_CN1	+	0.984			+	0.987
FS1_CC2	+	0.991	+	0.993	+	0.993
FS1_CN2	+	0.972	+	0.985	+	0.985
FS1_CC3			+	0.984	+	0.898
FS1_CN3			+	0.994	+	0.983
FS1_CC4			+	0.970	+	0.965
FS1_CN4			+	0.991	+	0.985
FS2_CC1	+	0.975			+	0.944
FS2_CN1	+	0.913		0.923	+	0.851
FS2_CC2			+	0.989	+	0.974
FS2_CN2			+	0.988	+	0.974
FS2_CC3			+	0.984	+	0.975
FS2_CN3			+	0.980	+	0.970
FS2_CC4	+	0.977			+	0.979
FS2_CN4	+	0.994			+	0.987
FS3_CC1	+	0.965	+	0.951	+	0.931
FS3_CN1	+	0.974	+	0.963	+	0.929
FS3_CC2	+	0.983			+	0.971
FS3_CN2	−				−	
FS3_CC3	+	0.974	+	0.972		
FS3_CN3	+	0.983	+	0.971		
FS1_BC1			+	0.989	+	0.984
FS1_BN1			+	0.978	+	0.945
FS1_BC2			+	0.992	+	0.982
FS1_BN2			+	0.817	+	0.732
FS1_BC3			+	0.994	+	0.994
FS1_BN3			+	0.978	+	0.974
FS1_BC4	+	0.994			+	0.994
FS1_BN4	+	0.930			+	0.900
FS2_BC1			+	0.993	+	0.981
FS2_BN1			+	0.971	+	0.832
FS2_BC2			+	0.987	+	0.968
FS2_BN2			+	0.983	+	0.957
FS2_BC3	+	0.994			+	0.991
FS2_BN3	+	0.990			+	0.982
FS2_BC4	+	0.993				
FS2_BN4	+	0.966				
FS3_BC1	+	0.979			+	0.957
FS3_BN1	+	0.985			+	0.952
FS3_BC2	+	0.987			+	0.981
FS3_BN2	+	0.983			+	0.931
FS3_BC3	+	0.977			+	0.968
FS3_BN3	+	0.969			+	0.912

*CC, colon cancer; CN, colon normal; BC, breast cancer; BN, breast normal; FF, fresh-frozen.
†+, Successfully assayed samples. −, Samples with which assay was attempted but failed.
‡R^2, correlation between expression profiles of technical replicates at the gene level.

of the array data are represented in Supplementary Tables 1–3 at http://ajp.amjpathol.org.

Array Data Normalization

Our method normalizes given array data with respect to reference data such as an average of multiple replicate arrays. We used cubic spline normalization that makes distributions of gene intensities on a given array and reference array similar. The normalization uses quantiles of sequence type signals to fit smoothing B-splines similar to what was proposed by Workman et al.[24]

Expression Data Analysis and Clustering Algorithm

To identify disease- and tissue-specific markers, we performed two separate analyses. 1) FFPE samples on Array Matrix 2 were distributed into the following group pairs:

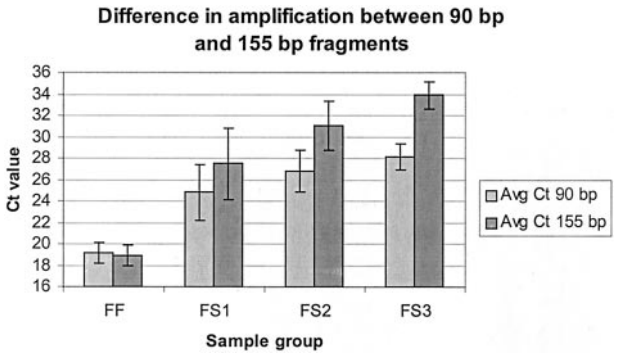

Figure 1. Real-time PCR analysis of RNAs isolated from FFPE tissues with different duration of storage. The Ct values (*y* axis) for two amplicons of different sizes that monitor a highly expressed gene, RPL13A, were plotted for each sample group (*x* axis): FF, fresh-frozen; FS1, 1 year; FS2, 2 years; FS3, 9–11 years. The average difference in the Ct values (ΔCt) of the two amplicons was derived from each sample group as −0.3 ± 0.1, 2.7 ± 1.1, 4.2 ± 1.1, and 5.8 ± 1.0, respectively. The **error bars** represent the SD from the mean.

colon normal versus colon cancer, breast normal versus breast cancer, and normal breast versus normal colon. We applied Mann-Whitney test with a *P* value cutoff of 0.01 and a twofold change requirement to identify marker genes using FFPE samples. 2) We divided fresh-frozen samples from Array Matrix 3 into colon cancer versus colon normal and breast cancer versus breast normal (two samples per group) and ran the algorithm using negative controls in combination with rank invariant set of probes for construction of an error model, as described by Fan et al.[18] Based on the array signals of selected genes, we computed the correlation coefficient matrix for the FFPE samples and clustered them using Agnes function in the *R* package with Ward's method. The markers identified from Array Matrix 2 were used to cluster FFPE samples on Array Matrix 1 while markers identified on Array Matrix 3 were applied to clustering FFPE samples from the same matrix.

Results

Quality of RNAs Isolated from FFPE Tissues with Different Durations of Storage

We used 8 fresh-frozen and 44 FFPE tissues (Table 1) with time of storage ranging from 1 year to over 10 years for this study. Total RNA was extracted from fresh-frozen and FFPE tissues and converted to cDNA (see Materials and Methods). Aliquots of the cDNA reactions were taken for real-time PCR analysis. To assess the integrity of RNA isolated from these FFPE tissues, we measured the amplification efficiency of two fragments (90 bp and 155 bp) from a highly expressed gene (RPL13A). As shown in Figure 1, the absolute Ct values increased with the storage time, correlating well with previous observations that RNA fragmentation increases with storage time.[17] In addition, a difference in threshold cycle (Ct) values was calculated by taking the average Ct value of duplicate samples for the amplification of the 90-bp fragment and subtracting the average Ct value for the amplification of the 155-bp fragment. The difference reflects the level of RNA degradation in the sample (ie, a bigger difference means more degraded). No difference in amplification efficiency was found in fresh-frozen samples, but the difference increased with the age of the archival samples from which the RNA was extracted, and was up to 6 cycle numbers in FFPE samples older than 10 years (Figure 1), indicating a high level of RNA degradation in these samples.

To obtain reproducible gene expression results, we used an RT-PCR test to pre-qualify the RNA samples before array analysis. RT-PCR primers were designed to target ~90-bp fragments in each of three housekeeping genes: UBC, HPRT, and PBDG. Of the 44 samples tested, only one sample (FS3-CN2) showed no amplification in RT-PCR even for the highly expressed ubiquitin C (UBC) gene. This sample also failed to produce any gene expression data on the array.

DASL Assay Performance and Reproducibility

We examined the impact of input RNA quantity on assay performance. Various amounts of total RNA (1000, 500, 250, and 100 ng) isolated from FFPE tissues were converted into cDNA. Each cDNA sample was split to perform two independent DASL assays. Highly reproducible results were obtained with as little as 50 ng of total RNA (R^2 = 0.97). More importantly, as shown in Figure 2, gene expression profiles generated with 50 ng (as well as 125 ng and 250 ng, data not shown) input RNA were quite comparable with those generated with 500 ng of RNA (R^2 = 0.95, on average). In standard clinical practice, it is always difficult to get exactly the same amount of RNA from different diseased tissues for study. Therefore, the relative insensitivity of the DASL assay to the amount of input RNA makes it readily adaptable to clinical settings.

We also compared the number of genes detectable by the DASL assay in 16 RNA samples extracted from paired fresh-frozen and FFPE colon and breast tissues, both cancerous and normal. More than 90% of the genes that were detected in the fresh-frozen samples were also detected in their matching FFPE samples, when 200 ng of total RNA was assayed. However, we observed that the gene expression profile of the paraffin-embedded samples had weaker correlation with the profile generated from the corresponding frozen samples (R^2 = 0.69), possibly due to sequence-dependent differences in mRNA degradation during tissue fixation and storage.

Lists of differentially expressed genes generated from fresh-frozen and FFPE samples had highly significant overlap (with the FFPE list containing ~50% less genes). For example, at a 0.01 confidence level, 64 of 231 genes were identified as differentially expressed in matching fresh-frozen samples (FS1_CC2: colon cancer versus FS1_CN2: colon normal), and 38 were differentially expressed in the corresponding FFPE samples. Twenty-eight of these genes were in common, which gives a significance of overlap of 1.0e-09, according to the Fisher's exact test,[25] applied to contingency tables formed from differential expression calls. For another matching

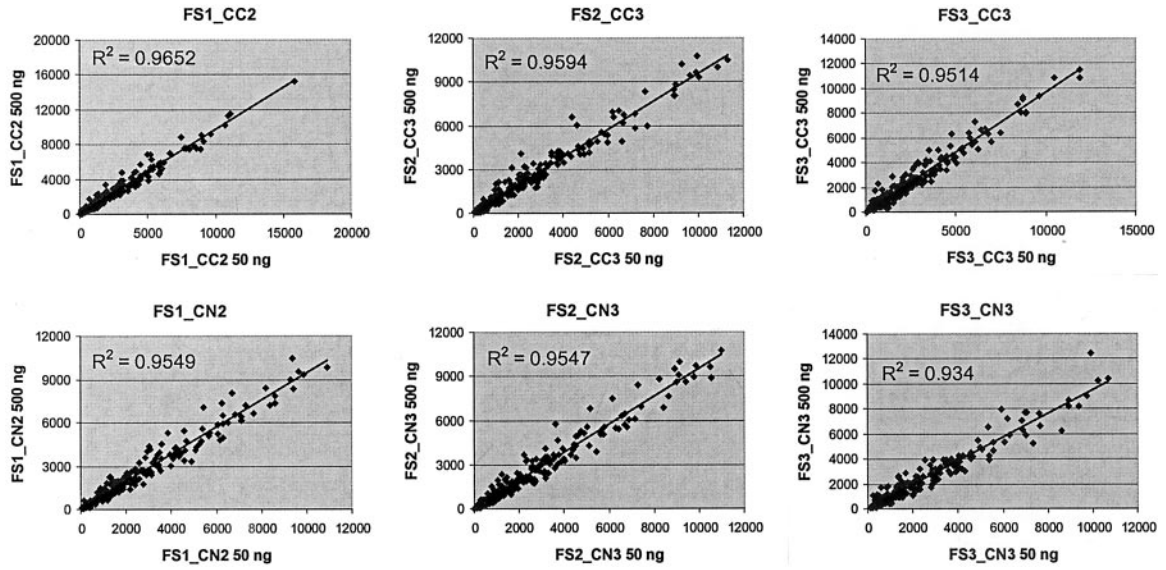

Figure 2. Reproducible expression profiling with various amounts of input RNA. The assay intensity for lower RNA input (50 ng, *x* axis) is plotted against the assay intensity for the same genes in the higher RNA input (500 ng, *y* axis) for six individual tissue samples.

pair, FS1_BC3: breast cancer versus FS1_BN3: breast normal, 61 genes were identified as differentially expressed using fresh-frozen and 33 using FFPE samples, with an overlap of 20 genes. The significance of this overlap is 3.8e-05. Together, these results suggest that sets of differentially expressed genes identified in FFPE samples resemble those identified from fresh-frozen samples.

All of the assays were done at a 1212-plex level, corresponding to 231 genes with 2 to 10 targeted sites per gene. This experimental design allowed assessment of the effect of the probe number on assay quantitation. Our subsampling analysis showed that three optimally designed probes performed comparably to four or more probes with regard to their ability to detect expressed genes as well as differential expression in RNA samples extracted from both fresh-frozen and FFPE tissues. Further lowering the probe number negatively impacted assay reproducibility. Probes optimized for fresh-frozen sample RNAs performed equally well with RNAs extracted from FFPE samples. Since DASL uses random priming in the cDNA synthesis, the probes can be designed to target any unique regions of the gene. There is no need to limit the selection of optimal probes to the 3′-end of the transcripts.

Cluster Analysis of Gene Expression Patterns in FFPE Samples

To further test the strategy of using archival tissues for cancer marker discovery, we generated expression profiles with paired (ie, "cancer versus normal" of same individual) fresh-frozen samples ($N = 4$ for each tissue type), and identified a subset of genes that distinguished cancer from normal tissues with a significant differential expression score ($P < 0.001$). 40 and 37 of these differentially expressed genes were identified from a set of 212 cancer-related genes for colon and breast tissue, respectively. Since we had a limited number of fresh-frozen samples (two for each class), our list could contain genes which simply reflect individual differences unrelated to cancer status. Expression profiles of these genes from FFPE samples ($N = 21$ for each tissue type) were then analyzed using an agglomerative nesting clustering method. The cancer and normal samples were separated into two distinct clusters in both of the tissue types; and cancer samples with the same clinical stage were clustered together (Figure 3). Only one breast cancer sample, FS3-BC3 (Table 1, ductal carcinoma *in situ*, Stage 0) was mis-clustered together with normal samples (Figure 3B), presumably because the selected cancer markers are specific for more advanced cancer stages, ie, not enough samples of this disease stage are represented in the sample set. As a matter of fact, FS3-BC3 was the only Stage 0 sample analyzed. All of the RNAs extracted from the FFPE samples were prequalified using a RT-PCR test (see above) before array analysis.

We also performed an alternate cluster analysis, in which genes selected by differential expression analysis from a set of 24 FFPE samples were used to cluster another set of 25 FFPE samples assayed independently in another experiment. The cluster analysis was done in two steps: first, genes distinguishing colon from breast tissue were selected. Based on these genes, we were able to separate samples from the second group into colon and breast tissue types with 100% accuracy. Second, genes specific for colon cancer and breast cancer were selected (similar to the analysis of the fresh-frozen samples). Based on these genes, colon cancer samples were separated from colon normal samples without mistake, while breast cancer samples were separated from breast normal samples with one mistake (FS3-BC3).

Based on cluster analyses of both fresh-frozen and FFPE samples assayed on Array Matrix 1 and 2, we

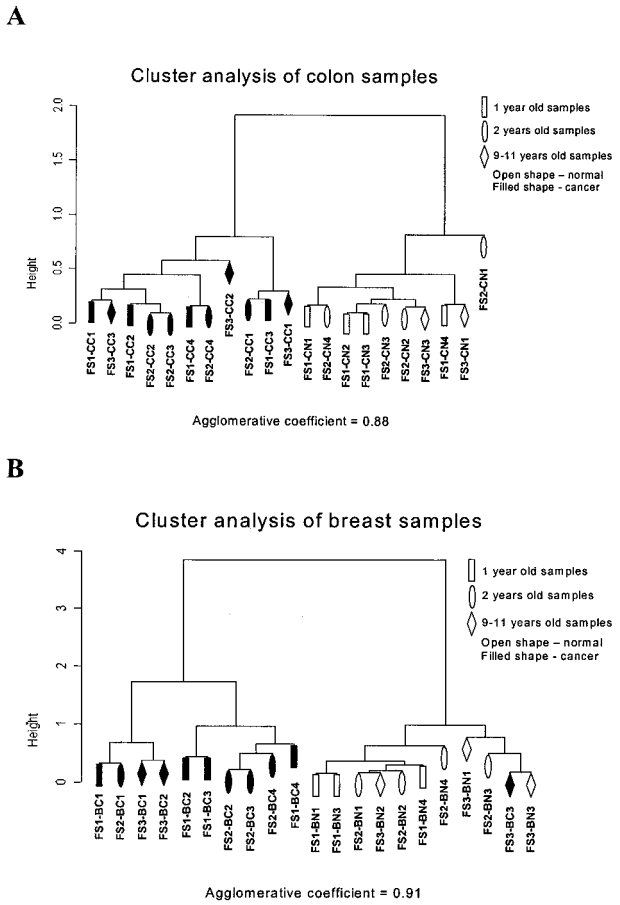

Figure 3. Cluster analysis of FFPE samples. Agglomerative clustering was based on the differentially expressed genes identified from fresh-frozen samples. The distance between subclusters (*y* axis, Height) measures the divergence of their expression profiles.

generated a list of differentially expressed genes that can distinguish colon cancer from colon normal tissue (SIM2, HAR, MMP7, FGFR2, TMEPAI, CLU, PLAB, and human skin collagenase) and a list of genes that can distinguish breast cancer from breast normal tissue (HAR, FGF2, calmegin, IGF-1a, MET, EGFR, ITGA6, IGF2, and BMPR1B), each at a P value <0.01. We plotted the array data for some of these genes—four for each tissue type (Figure 4). Some of them were previously reported as differentially expressed in solid tumors. For example, certain FGFR2 isoforms were previously reported as downregulated in 60% of prostate tumors;[26] PLAB (MIC-1) was shown to be overexpressed in gastric tumor tissues;[27] loss of FGF2 expression was associated with malignant progression in breast; [28] increased IGF-I level in breast cancer epithelial cells was linked to lower degree of malignancy;[29] and EGFR (ERBB1) was underexpressed in 82% of breast tumors compared to normal breast tissue.[30] One of the genes which we identified as differentially expressed in the cancer and normal colon tissues was SIM2, a gene previously characterized as a solid tumor marker.[31,32] Together, these results demonstrate that it should be possible to identify robust gene expression signatures in FFPE samples using an array-based approach and standard classification algorithms.

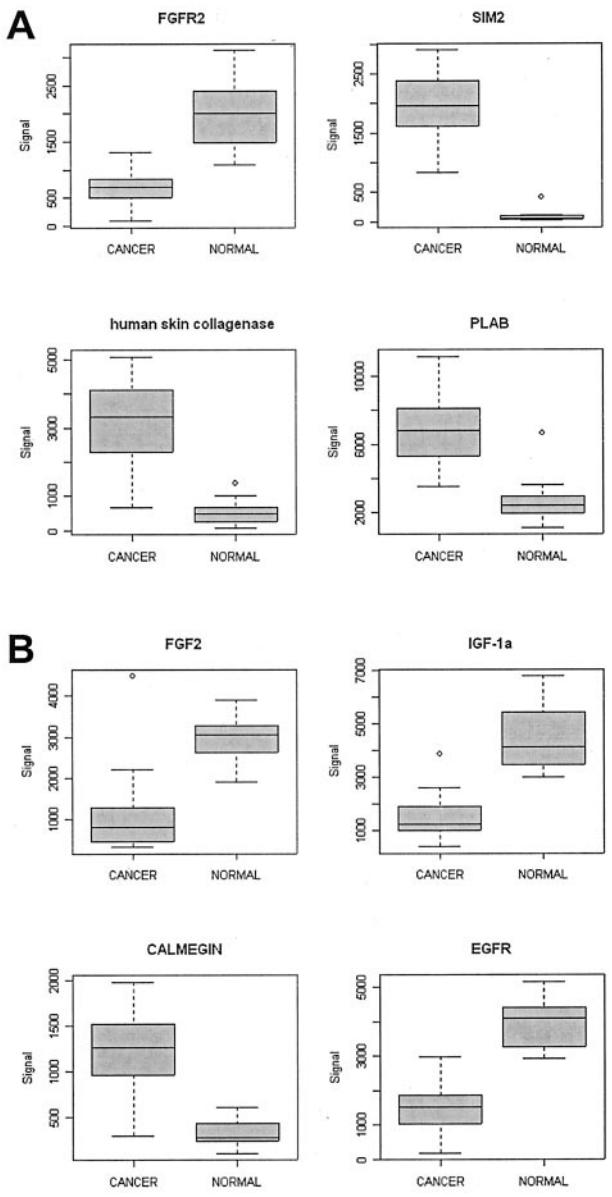

Figure 4. Box plots of the array data for selected cancer-specific markers. Array intensities (*y* axis) were calculated for the four colon cancer markers (**A**) and the four breast cancer markers (**B**) from both fresh-frozen and FFPE sample analysis. For the colon cancer markers (**A**), 12 cancer and 12 normal tissues were used. For the breast cancer markers (**B**), 11 cancer and 11 normal tissues were used. 500 ng of total RNA isolated from the FFPE tissue blocks were used in each assay. The **black bar** represents the mean intensity value. The **gray box** defines quartiles (25% and 75%, respectively). The **error bars** are upper and lower adjacent limits (median ± 1.5*IQR). **Dots** represent the outliers. The *P* values for the colon cancer markers are 7.40E-07 (SIM2), 0.0005 (PLAB), 0.0014 (FGFR2), and 0.0015 (human skin collagenase). The *P* values for the breast cancer markers are 0.0002 (EGFR), 0.0010 (IGF-1a), 0.0035 (FGF2), and 0.0063 (calmegin).

Furthermore, seven colon cancer and four breast cancer-specific markers identified from the array analysis were tested by qPCR with 46 individual samples (4 fresh-frozen and 20 FFPE colon tissues, and 4 fresh-frozen and 18 FFPE breast tissues). Good correlations between the threshold cycle (Ct) number and the array intensity for the 11 markers was obtained with the fresh-frozen samples ($R^2 = 0.88$). However, poor correlations were observed with the FFPE samples ($R^2 = 0.41$), mainly because the

qPCR assay was less reproducible and less sensitive in these samples. Individual FFPE samples are known to have different degrees of RNA degradation,[17] which in turn dramatically affect the qPCR results (Figure 1). It was previously reported, that to obtain faithful qPCR results in FFPE samples, normalization based on multiple housekeeping genes has to be used to correct for differences arising from variability in RNA quality and total quantity of RNA in each assay.[17] Despite the poor quality of qPCR data from FFPE samples, a consistent general trend was observed, where low Ct numbers correlate well with the higher array intensity in these samples (data not shown).

Discussion

RNA from FFPE specimens can be difficult to extract, since the RNA becomes cross-linked and degraded during the fixation and storage process; in addition, the amount of tumor tissue in the FFPE specimen is often very small. Therefore, it is essential to have a robust method to retrieve high quality RNA from FFPE tissue efficiently. There are various commercially available RNA extraction kits for this purpose, but their comparison was not a goal of this study. With our current protocol, similar expression profiles were obtained with RNAs extracted independently from the same paraffin tissue blocks ($R^2 = 0.93$). To prequalify the RNA samples before array analysis, we used a real-time PCR-based method to assess the intactness of the RNA samples (Figure 1). Of the 44 samples used in this study, only one (FS3-CN2) failed the test. We found this approach more effective than using a combination of RNA quantitation and a gel-based size analysis.

The DASL assay combines the advantages of array-based gene expression analysis with those of multiplexed qPCR,[18] thereby offering much higher multiplexing capacity and huge throughput and cost-saving advantages. It uses as little as 50 ng of total RNA to analyze 300 to 400 genes in FFPE samples, ~100-fold less than what is required by qPCR, which usually uses 20 to 50 ng per reaction (per gene). The assay is highly reproducible (see Figure 2 and Supplementary Table 1 at http://ajp.amjpathol.org). Since many genes are measured simultaneously in one DASL assay, it provides an excellent internal data normalization, thus solving a major problem encountered by qPCR. This becomes very important when cross-sample comparisons are needed, especially when the samples under study have different degrees of RNA degradation.

Our results show that we can obtain reproducible gene expression profiles with FFPE samples older than 10 years. 90% of the genes detected in fresh-frozen sample RNA were detected with RNA from matching FFPE samples. Gene expression profiles of the FFPE samples do not exactly correlate with those from the fresh-frozen samples ($R^2 = 0.69$), presumably because of different rates of RNA degradation occurring during the fixation and paraffin embedding process and during storage.[9] However, gene expression analysis within FFPE samples should provide a powerful approach to discover molecular signatures associated with a given disease state, or histological or clinical phenotypes. This technology is especially useful for determining cancer prognosis or therapy response, because it allows not only prospective analysis but also retrospective analysis. Using DASL, gene expression analysis can now be performed on routinely stored tumor specimens from patients with known outcomes. Our results showed that characteristic gene expression patterns can be identified in FFPE samples for a particular cancer type (Figure 3). We are currently working on a prostate cancer prognosis project that is to search for specific molecular markers that correlate with the following clinical parameters: cancer classification, tumor grade or tumor stage, organ confined disease versus locally advanced tumors, therapeutic response, and overall prognosis. The main tissues for study are archived prostate carcinomas ($N = 240$) and benign hyperplastic prostates ($N = 60$) with at least 5 years of clinical follow-up.

We also demonstrated the utility of this strategy by validating eight tissue and cancer-specific markers identified previously from fresh-frozen samples using Affymetrix GeneChip microarrays. The eight genes were assayed along with other 212 cancer-related genes in 51 fresh-frozen and FFPE samples including 26 breast and 25 colon tissues (Table 1). All four tissue-specific markers were able to correctly identify the tissue of origin with a typical tissue-specific expression pattern, and the cancer specific markers were highly expressed in the tumor samples and had significantly lower levels of expression in the matching normal tissues (data not shown). Furthermore, the marker sensitivity and specificity measured by the array analysis were compared to those determined for qPCR with a subset ($N = 36$) of the FFPE samples. Overall, the array analysis outperformed qPCR.

The DASL assay is a powerful technology for high-throughput expression profiling of hundreds of genes in hundreds to thousands of samples.[18] We have now shown that the DASL assay can be applied to clinical FFPE samples, an important source of material that has not been amenable to conventional microarray-based assays. This opens up the possibility of a new generation of microarray-based gene expression assays being applicable not only to routine clinical care but also to the retrospective analysis of paraffin-embedded sample collections obtained during clinical trials or from large population-based cohorts.

Acknowledgments

We thank Philippe Rigault, Lixin Zhou, and Ivan Mikoulitch for assistance with assay probe design and data analysis.

References

1. Lockhart DJ, Dong H, Byrne MC, Follettie MT, Gallo MV, Chee MS, Mittmann M, Wang C, Kobayashi M, Horton H, Brown EL: Expression monitoring by hybridization to high-density oligonucleotide arrays. Nature Biotechnol 1996, 14:1675–1680
2. Golub TR, Slonim DK, Tamayo P, Huard C, Gaasenbeek M, Mesirov

JP, Coller H, Loh ML, Downing JR, Caligiuri MA, Bloomfield CD, Lander ES: Molecular classification of cancer: class discovery and class prediction by gene expression monitoring. Science 1999, 286: 531–537
3. Perou CM, Sorlie T, Eisen MB, van de Rijn M, Jeffrey SS, Rees CA, Pollack JR, Ross DT, Johnsen H, Akslen LA, Fluge O, Pergamenschikov A, Williams C, Zhu SX, Lonning PE, Borresen-Dale AL, Brown PO, Botstein D: Molecular portraits of human breast tumours. Nature 2000, 406:747–752
4. Welsh JB, Sapinoso LM, Su AI, Kern SG, Wang-Rodriguez J, Moskaluk CA, Frierson HF, Jr., Hampton GM: Analysis of gene expression identifies candidate markers and pharmacological targets in prostate cancer. Cancer Res 2001, 61:5974–5978
5. Dhanasekaran SM, Barrette TR, Ghosh D, Shah R, Varambally S, Kurachi K, Pienta KJ, Rubin MA, Chinnaiyan AM: Delineation of prognostic biomarkers in prostate cancer. Nature 2001, 412:822–826
6. van 't Veer LJ, Dai H, van de Vijver MJ, He YD, Hart AA, Mao M, Peterse HL, van der Kooy K, Marton MJ, Witteveen AT, Schreiber GJ, Kerkhoven RM, Roberts C, Linsley PS, Bernards R, Friend SH: Gene expression profiling predicts clinical outcome of breast cancer. Nature 2002, 415:530–536
7. West M, Blanchette C, Dressman H, Huang E, Ishida S, Spang R, Zuzan H, Olson JA Jr, Marks JR, Nevins JR: Predicting the clinical status of human breast cancer by using gene expression profiles. Proc Natl Acad Sci USA 2001, 98:11462–11467
8. Lewis F, Maughan NJ, Smith V, Hillan K, Quirke P: Unlocking the archive—gene expression in paraffin-embedded tissue. J Pathol 2001, 195:66–71
9. Godfrey TE, Kim SH, Chavira M, Ruff DW, Warren RS, Gray JW, Jensen RH: Quantitative mRNA expression analysis from formalin-fixed, paraffin-embedded tissues using 5′ nuclease quantitative reverse transcription-polymerase chain reaction. J Mol Diagn 2000, 2:84–91
10. Karsten SL, Van Deerlin VM, Sabatti C, Gill LH, Geschwind DH: An evaluation of tyramide signal amplification and archived fixed and frozen tissue in microarray gene expression analysis. Nucleic Acids Res 2002, 30:E4
11. Abrahamsen HN, Steiniche T, Nexo E, Hamilton-Dutoit SJ, Sorensen BS: Towards quantitative mRNA analysis in paraffin-embedded tissues using real-time reverse transcriptase-polymerase chain reaction: a methodological study on lymph nodes from melanoma patients. J Mol Diagn 2003, 5:34–41
12. Lehmann U, Bock O, Glockner S, Kreipe H: Quantitative molecular analysis of laser-microdissected paraffin-embedded human tissues. Pathobiology 2000, 68:202–208
13. Daigo Y, Chin SF, Gorringe KL, Bobrow LG, Ponder BA, Pharoah PD, Caldas C: Degenerate oligonucleotide primed-polymerase chain reaction-based array comparative genomic hybridization for extensive amplicon profiling of breast cancers: a new approach for the molecular analysis of paraffin-embedded cancer tissue. Am J Pathol 2001, 158:1623–1631
14. Palmieri G, Ascierto PA, Cossu A, Mozzillo N, Motti ML, Satriano SM, Botti G, Caraco C, Celentano E, Satriano RA, Lissia A, Tanda F, Pirastu M, Castello G: Detection of occult melanoma cells in paraffin-embedded histologically negative sentinel lymph nodes using a reverse transcriptase polymerase chain reaction assay. J Clin Oncol 2001, 19:1437–1443
15. Specht K, Richter T, Muller U, Walch A, Werner M, Hofler H: Quantitative gene expression analysis in microdissected archival formalin-fixed and paraffin-embedded tumor tissue. Am J Pathol 2001, 158: 419–429
16. Lehmann U, Glockner S, Kleeberger W, von Wasielewski HF, Kreipe H: Detection of gene amplification in archival breast cancer specimens by laser-assisted microdissection and quantitative real-time polymerase chain reaction. Am J Pathol 2000, 156:1855–1864
17. Cronin M, Pho M, Dutta D, Stephans JC, Shak S, Kiefer MC, Esteban JM, Baker JB: Measurement of gene expression in archival paraffin-embedded tissues: development and performance of a 92-gene reverse transcriptase-polymerase chain reaction assay. Am J Pathol 2004, 164:35–42
18. Fan JB, Yeakley JM, Bibikova M, Chudin E, Wickham E, Chen J, Doucet D, Rigault P, Zhang B, Shen R, McBride C, Li HR, Fu XD, Oliphant A, Barker DL, Chee MS: A versatile assay for high-throughput gene expression profiling on universal array matrices. Genome Res 2004, 14:878–885
19. Phillips J, Eberwine JH: Antisense RNA amplification: a linear amplification method for analyzing the mRNA population from single living cells. Methods 1996, 10:283–288
20. Barker DL, Theriault G, Che D, Dickinson T, Shen R, Kain R: Self-assembled random arrays: high-performance imaging and genomics applications on a high-density microarray platform. Proc SPIE 2003, 4966:1–11
21. Fan JB, Oliphant A, Shen R, Kermani B, Garcia F, Gunderson K, Hansen M, Steemers F, Butler SL, Deloukas P, Galver L, Hunt S, McBride C, Bibikova M, Chen J, Wickham E, Doucet D, Chang W, Campbell D, Zhang B, Kruglyak S, Bentley D, Haas J, Rigault P, Zhou L, Stuelpnagel J, Chee MS: Highly parallel SNP genotyping. Cold Spring Harbor Symposia on Quantitative Biology 2003, 68:69–78
22. Gunderson KL, Kruglyak S, Graige MS, Garcia F, Kermani B, Zhao C, Che D, Dickinson T, Wickham E, Bierle J, Doucet D, Milewski M, Yang R, Siegmund C, Haas J, Zhou L, Oliphant A, Fan JB, Barnard S, Chee MS: Decoding Randomly Ordered DNA Arrays. Genome Res 2004, 14:870–877
23. Galinsky VL: Automatic registration of microarray images. II. Hexagonal grid. Bioinformatics 2003, 19:1832–1836
24. Workman C, Jensen LJ, Jarmer H, Berka R, Gautier L, Nielser HB, Saxild HH, Nielsen C, Brunak S, Knudsen S: A new non-linear normalization method for reducing variability in DNA microarray experiments. Genome Biol 2002, 3:research0048
25. Weisstein EW: Fisher's Exact Test: From MathWorld–A Wolfram Web Resource: http://mathworld.wolfram.com/FishersExactTest.html., 1999
26. Naimi B, Latil A, Fournier G, Mangin P, Cussenot O, Berthon P: Down-regulation of (IIIb) and (IIIc) isoforms of fibroblast growth factor receptor 2 (FGFR2) is associated with malignant progression in human prostate. Prostate 2002, 52:245–252
27. Lee DH, Yang Y, Lee SJ, Kim KY, Koo TH, Shin SM, Song KS, Lee YH, Kim YJ, Lee JJ, Choi I, Lee JH: Macrophage inhibitory cytokine-1 induces the invasiveness of gastric cancer cells by up-regulating the urokinase-type plasminogen activator system. Cancer Res 2003, 63: 4648–4655
28. Liu D, Buluwela L, Ali S, Thomson S, Gomm JJ, Coombes RC: Retroviral infection of the FGF2 gene into MCF-7 cells induces branching morphogenesis, retards cell growth and suppresses tumorigenicity in nude mice. Eur J Cancer 2001, 37:268–280
29. Eppler E, Zapf J, Bailer N, Falkmer UG, Falkmer S, Reinecke M: IGF-I in human breast cancer: low differentiation stage is associated with decreased IGF-I content. Eur J Endocrinol 2002, 146:813–821
30. Bieche I, Onody P, Tozlu S, Driouch K, Vidaud M, Lidereau R: Prognostic value of ERBB family mRNA expression in breast carcinomas. Int J Cancer 2003, 106:758–765
31. Deyoung MP, Scheurle D, Damania H, Zylberberg C, Narayanan R: Down's syndrome-associated single minded gene as a novel tumor marker. Anticancer Res 2002, 22:3149–3157
32. DeYoung MP, Tress M, Narayanan R: Identification of Down's syndrome critical locus gene SIM2-s as a drug therapy target for solid tumors. Proc Natl Acad Sci USA 2003, 100:4760–4765